nature communications

Article

https://doi.org/10.1038/s41467-025-56741-w

Biological age model using explainable automated CT-based cardiometabolic biomarkers for phenotypic prediction of longevity

Received: 22 July 2024

Accepted: 23 January 2025

Published online: 07 February 2025

Check for updates

Perry J. Pickhardt[1,2] ✉, Michael W. Kattan[3], Matthew H. Lee[1], B. Dustin Pooler[1], Ayis Pyrros[4,5], Daniel Liu[1], Ryan Zea[1], Ronald M. Summers[6] & John W. Garrett[1,2]

We derive and test a CT-based biological age model for predicting longevity, using an automated pipeline of explainable AI algorithms that quantifies skeletal muscle, abdominal fat, aortic calcification, bone density, and solid abdominal organs. We apply these AI tools to abdominal CT scans from 123,281 adults (mean age, 53.6 years; 47% women; median follow-up, 5.3 years). The final weighted CT biomarker selection was based on the index of prediction accuracy. The CT model significantly outperforms standard demographic data for predicting longevity (IPA = 29.2 vs. 21.7; 10-year AUC = 0.880 vs. 0.779; $p < 0.001$). Age- and sex-corrected survival hazard ratio for the highest-vs-lowest risk quartile was 8.73 (95% CI,8.14-9.36) for the CT biological age model, and increased to 24.79 after excluding cancer diagnoses within 5 years of CT. Muscle density, aortic plaque burden, visceral fat density, and bone density contributed the most. Here we show a personalized phenotypic CT biological age model that can be opportunistically-derived, regardless of clinical indication, to better inform risk assessment.

The aging process reflects the inexorable structural and functional decline of an organism[1], although the specific mortality risk over time can widely vary according to a host of genetic and environmental modifiers. Historically, chronological age and sex have driven many healthcare decisions regarding prevention, screening, and intervention. However, chronological age represents an incomplete and fallible measure of health status (or "healthspan") and longevity, and there is growing public awareness that other contributing factors should be considered[2–4]. Biological age (BA) is a potentially useful construct that attempts to reflect the cumulative physiologic effect of lifestyle habits, genetic predisposition, and superimposed disease processes beyond simply the number of years lived. Attempts at deriving an effective BA date back at least half a century[5], but with only limited success. Much of the current geroscience focus to date for attempting to derive an effective BA has centered on various "frailomics" at the cellular and subcellular levels, including (epi)genomics (eg, telomere length and epigenetic clock), proteomics, and metabolomics, as well as various other laboratory and clinical measures[1,6–9].

Imaging biomarkers have generally received less attention for estimating BA[7,8], but arguably may better reflect the cumulative

[1]The Department of Radiology, University of Wisconsin School of Medicine & Public Health, Madison, WI, USA. [2]The Department of Medical Physics, University of Wisconsin School of Medicine & Public Health, Madison, WI, USA. [3]The Department of Quantitative Health Sciences, Cleveland Clinic, Cleveland, OH, USA. [4]Department of Radiology, Duly Health and Care, Downers Grove, IL, USA. [5]Department of Biomedical and Health Information Sciences, University of Illinois-Chicago, Chicago, IL, USA. [6]Imaging Biomarkers and Computer-Aided Diagnosis Laboratory, Radiology and Imaging Sciences, National Institutes of Health Clinical Center, Bethesda, MD, USA. ✉e-mail: ppickhardt2@uwhealth.org

macroscopic effects of aging at the tissue and organ levels. In particular, abdominal computed tomography (CT) represents an appealing candidate for a more personalized investigation. Specifically, CT can provide an objective, understandable, and reproducible assessment of internal tissue composition, including quantitative measures of skeletal muscle, abdominal fat, vascular calcification, bone density, and other organs[10,11]. When combined, these CT-based cardiometabolic biomarkers may better reflect the combined phenotypical characteristics that result from the interaction of one's genotype with environmental factors and lifestyle. In particular, CT can reveal findings of silent, pre-symptomatic disease processes such as osteoporosis, atherosclerosis, sarcopenia, and metabolic syndrome, potentially allowing for earlier preventive action[12–17]. Consequently, these CT-based measures have been shown to correlate with aging and survival[13]. Furthermore, the once arduous task of manually deriving these CT biomarkers has been replaced by "explainable" or understandable artificial intelligence (AI) algorithms that are rapid and indefatigable[18]. Unlike other frailomic approaches, these CT-based cardiometabolic biomarkers can be derived retrospectively (or prospectively), regardless of the clinical indication, including scans performed many years earlier to allow for both "snapshots in time" and for built-in longitudinal follow-up for survival analysis[10]. Given that CT scans are the most frequently performed abdominal imaging test in middle-age and older adults[19], the opportunity already exists to leverage or repurpose this body composition data for general health assessment[10,18].

The purpose of this study was to derive an abdominal CT-based biological age (CTBA) model informed only by an automated pipeline of validated cardiometabolic biomarkers and compare survival prediction over the usual demographic input data of chronological age, sex, and race.

Results

The final study cohort consisted of 123,281 adults (mean age 53.6 years [SD 17.4]; 58,308 [47%] women and 64,973 [53%] men) who underwent abdominal CT scanning over a 20-year time interval. Median clinical post-CT follow-up was 5.3 years and more than one-quarter of all patients had over a decade of follow-up (IQR, 1.9-10.4 years). A total of 26,554 (22%) patients died over the post-CT follow-up interval, whereas the remaining 96,727 (78%) were alive at last verifiable clinical contact. The median post-CT clinical follow-up interval was 6.0 years [IQR 2.6–11.3] for individuals still alive at last contact, and 2.6 years [IQR 0.7–6.8] for those who died. By race, the patient cohort was predominately White (92%), followed by Black (5%), Asian (2%), American Indian (1%), and Hawaiian (<1%) descent.

From the full panel of potential automated CT measures (Fig. 1), a total of eight biomarkers contributed sufficiently to the CTBA model to warrant inclusion. Of these, muscle density, abdominal aortic calcium score, visceral fat density, bone density, and visceral-to-subcutaneous fat ratio demonstrated the largest IPA drop, signifying the greatest contribution to the CTBA model. A patient example is shown in Fig. 2. The final panel of CT biomarkers, including their drop in IPA values, are shown in Table 1, along with the results of the demographics model utilizing patient chronological age, sex, and race. As expected, the demographics model was largely driven by chronological age, to which the CTBA model is blinded. For the full CTBA model, the index of prediction accuracy (or IPA) was 29.2, compared with an IPA of 21.7 for the demographics (chronological age/sex/race) model ($p < 0.001$). A nomogram for predicting survival according to the CTBA model is shown in Fig. 3, as well as a scatter plot for individual survival prediction by the CTBA model.

Skeletal muscle density was the dominant CT biomarker in the survival model, whereas muscle area played only a minor role. In terms of ROC curve analysis, the 5-year and 10-year AUCs for the CTBA model were 0.890 (95% CI, 0.884–0.896) and 0.880 (95% CI, 0.875–0.885), respectively, compared with 0.784 (95% CI, 0.776–0.792) and 0.782 (95% CI, 0.776–0.788) using patient CA, sex, and race, respectively ($p < 0.001$). For BMI, 5-year and 10-year AUCs were 0.520 (95% CI, 0.509–0.532) and 0.536 (95% CI, 0.526-0.546), respectively. For most CT biomarkers used in the CTBA model, substantial differences were observed between patients who died versus survived during their clinical follow-up. For example, Table 2 shows the difference in these

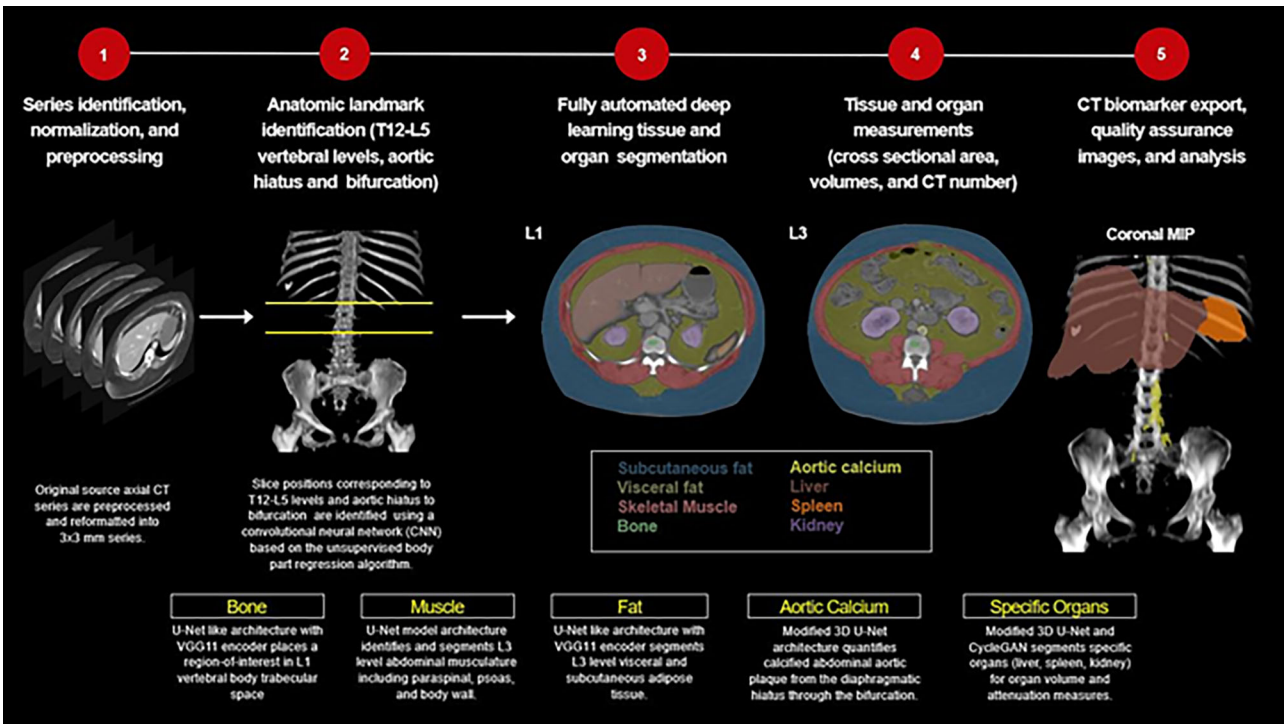

Fig. 1 | Overview of the CT-based AI pipeline. Schematic flowchart of AI pipeline for the fully automated CT body composition biomarkers.

https://doi.org/10.1038/s41467-025-56741-w

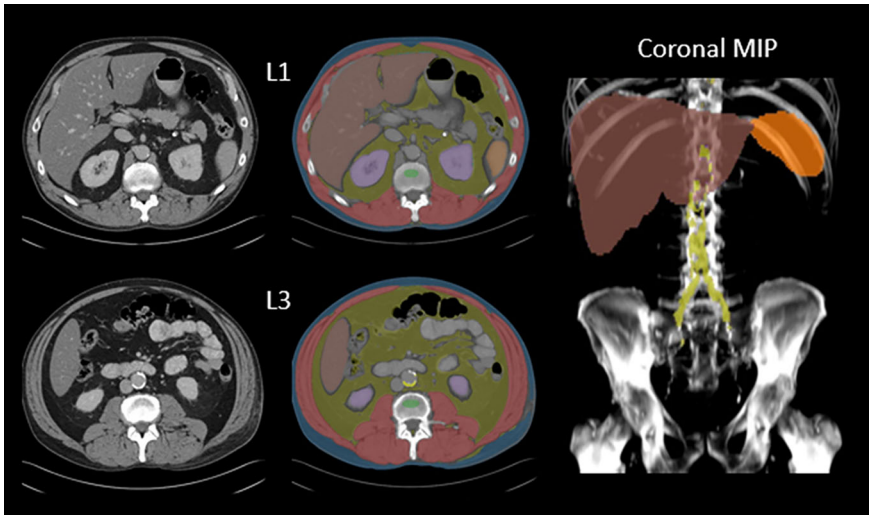

Fig. 2 | Middle-age adult patient who underwent CT for nonspecific abdominal pain (Case example from the primary cohort). Axial images from abdominal CT at the L1 and L3 vertebral levels (left), with the corresponding axial (middle) and coronal MIP (right) QA images automatically derived from the AI biomarker tools. This patient had no relevant past medical history except for hypertension. Beyond hepatic steatosis, the scan was interpreted as normal. Ten months after CT, the patient suffered an acute myocardial infarction and underwent emergent coronary artery bypass. The patient then suffered a stroke five years later and died prematurely three years after that (9.2 years after CT). According to the CTBA model, the patient was within the highest-risk quartile and had a predicted 10-year survival of 49% from the time of CT. Many key CT biomarkers contributing to the CTBA model were abnormal (see Table 3 for comparison): muscle density = 32.9 HU, aortic Agatston score = 12,342, visceral fat density = -88.7 HU, trabecular bone density = 110.0 HU, and visceral-to-subcutaneous fat ratio (VSR) = 1.99. All of these CT biomarkers were in the 66th-99th percentile for middle-aged men, with VSR at the 92nd percentile and aortic Agatston score at the 99th percentile.

Table 1 | Model results according to drop in index of predictive accuracy (IPA)

CTBA Model:	
Full Model IPA = 29.2	
Automated CT Biomarker*	**Drop in IPA****
Skeletal muscle density	5.1
Aortic calcium score	2.0
Visceral adipose tissue density	1.5
L1 trabecular bone density	1.1
Visceral-to-subcutaneous fat ratio (VSR)	0.4
Kidney volume	0.3
Subcutaneous adipose tissue area	0.2
Skeletal muscle area	0.1
Demographics Model:	
Full Model IPA = 21.7	
Demographic measure	**Drop in IPA****
Chronological age	21.1
Sex	0.3
Race	0.1

*CT biomarkers with an IPA-drop <0.1 were excluded from the final model.
**A larger IPA-drop signifies a greater contribution to the model prediction results.

biomarker measures for patients who died within 5 years after CT versus those who survived at least 5 years after CT, according to age group and sex. Neither the hepatic nor splenic biomarkers contributed to the final CTBA model, with a drop in IPA values < 0.1.

A Kaplan-Meier plot according to CTBA model output quartiles for the full study cohort is shown in Fig. 4. The age- and sex-corrected survival HR for the highest versus lowest risk CTBA quartile was 8.73 (95% CI, 8.14–9.36). When comparing the highest risk against the other three quartiles, the age- and sex-corrected HR was 3.13 (95% CI, 3.04–3.23). Kaplan-Meier plots subcategorized by patient sex (males and females), middle age (40–59 years), and older age (60–79 years) are shown in Fig. 5. To mitigate the risk of immediate mortality bias, we repeated the analysis after excluding patients diagnosed with cancer within 5 years of CT and after excluding patients who died within 2 years of CT. Accordingly, the age- and sex-corrected survival HRs for the highest-vs-lowest risk CTBA quartile increased to 24.79 after excluding cancer and 17.06 after excluding imminent death. Table 3 provides more complete AUC and HR results for the total cohort and sub-cohorts. To further reduce the influence of patient age on the model performance, we performed sub-analyses according to 5-year intervals; results are shown in Table 4 and Supplementary Fig. 1. An example case is shown in Fig. 2 for a patient in the highest-risk CTBA quartile.

External validation cohort

The final study group for the external validation cohort consisted of 40,718 adults (mean age 53.9 years [SD 16.9]; 22,316 [55%] women and 18,402 [45%] men) who underwent abdominal CT over a 20-year time interval. Median clinical post-CT follow-up was 5.3 years (IQR, 2.9–8.8 years), consisting of 253,298 total person-years of follow-up. A total of 3718 (9%) patients died over the post-CT follow-up interval, whereas the remaining 37,000 (91%) were alive at last verifiable contact. The median post-CT clinical follow-up interval was 5.4 years [IQR 3.1–9.0] for individuals still alive at last contact, and 3.5 years [IQR 1.4–6.9] for those who died. According to race, the patient cohort was predominately White (89%), followed by Black (5%), Asian (6%), American Indian (<1%), and Hawaiian (<1%) descent.

The CTBA model performed similarly well on the external validation cohort, with a full model IPA of 28.6, compared with 18.5 for the demographics model. A calibration plot of the CTBA model on this external cohort is shown in Fig. 6. The 5-year and 10-year AUC values were 0.893 (95% CI, 0.867–0.918) and 0.888 (95% CI, 0.869–0.908), respectively. A Kaplan-Meier survival plot for the external validation cohort based on CTBA model quartiles is shown in Fig. 6. The age- and sex-corrected survival HR for the highest-vs-lowest risk CTBA quartile was 5.14 (95% CI, 3.98–6.63). When comparing the highest-risk against the other three quartiles, the age- and sex-corrected HR was 2.45 (95% CI, 2.24–2.69).

https://doi.org/10.1038/s41467-025-56741-w

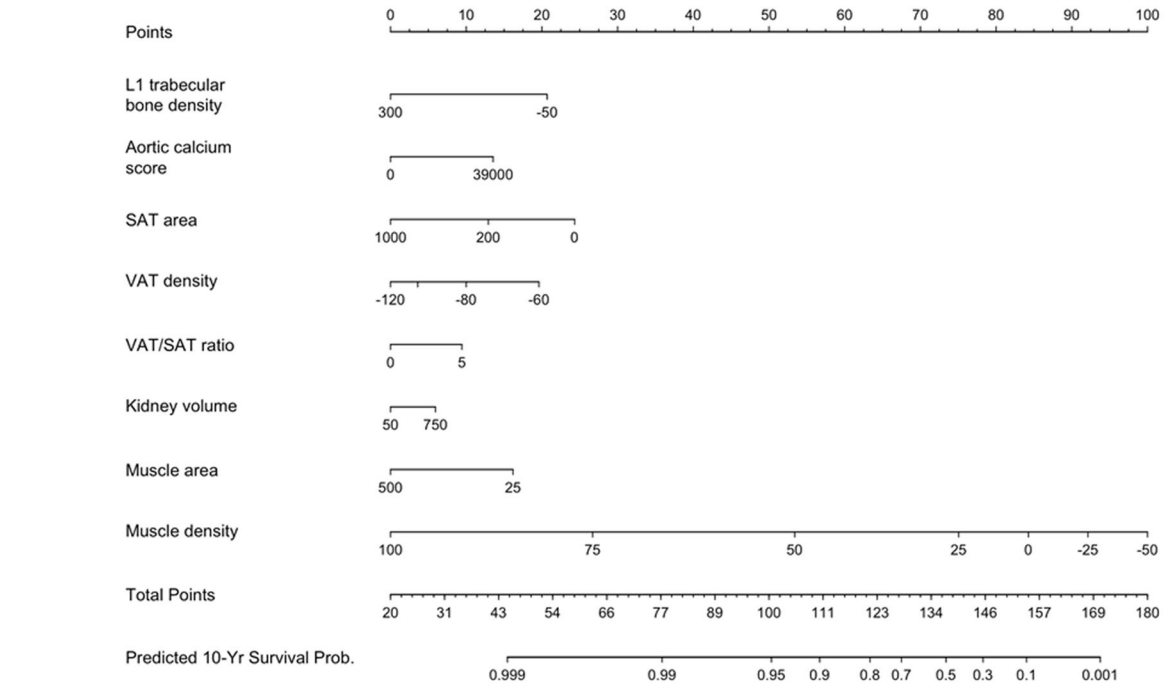

A.

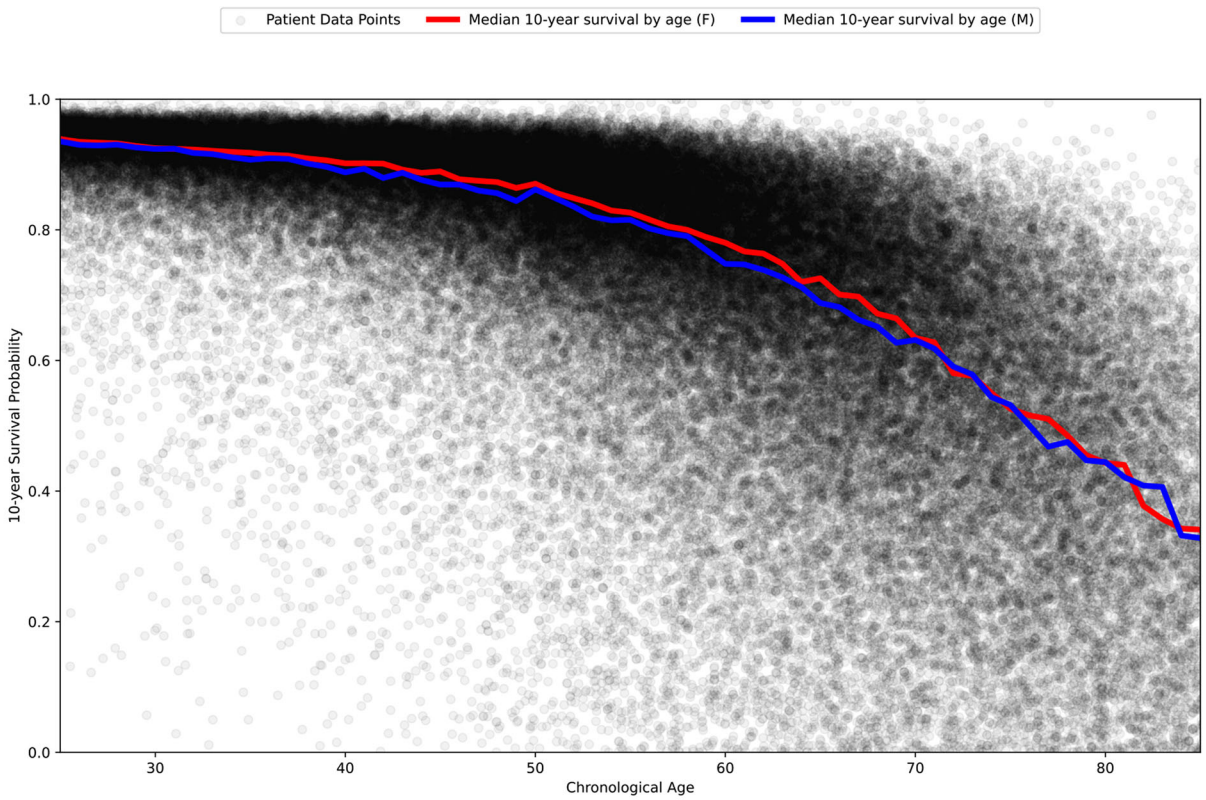

B.

Fig. 3 | Nomogram and scatter plot for CT biological age (CTBA) model for predicting survival. A For each CT biomarker, points are assigned according to a vertical line through the specific biomarker value and the points scale at the top. After summing the points for each predictor, the total points then correspond to a survival probability at the bottom. Note the dominant potential contribution related to muscle density. **B** Individual patient data points for predicted mortality risk are displayed according to chronological age, to which the model was blinded. Solid red (women) and blue (men) lines indicate the overall median predicted 10-year survival probability based on the CTBA model.

https://doi.org/10.1038/s41467-025-56741-w

Table 2 | CT body composition biomarker metrics according to 5-year post-CT survival horizon*

Sex	Age* (years)	Muscle Density (HU)		Abdominal Aortic Calcium Score (Agatston)		Visceral Fat Density(HU)		Trabecular Bone Density (HU)		Visceral-to-Subcutaneous Fat Ratio (VSR)		Kidney Volume(mL)		Subcutaneous Fat Area (cm²)		Muscle Area(cm²)		Patient N	
		Alive	Dead	Alive	Dead	Alive	Dead	Alive	Dead	Alive	Dead	Alive	Dead	Alive	Dead	Alive	Dead	Alive	Dead
Men	18–39	48 (41–53)	44 (36–49)	0 (0–0)	0 (0–0)	−90 (−97–82)	-89 (-96–82)	167 (145–192)	166 (146–189)	0.63 (0.42–0.90)	0.70 (0.51–0.98)	424 (374–485)	419 (338–489)	150 (83–237)	155 (80–241)	181 (160–203)	182 (152–203)	6169	292
	40–59	40 (32–45)	34 (25–41)	0 (0–117)	65 (0–885)	−95 (−100–88)	−90 (−98–82)	144 (124–165)	138 (115–161)	1.02 (0.72–1.43)	1.02 (0.69–1.46)	445 (386–514)	442 (368–528)	179 (129–250)	176 (120–252)	188 (169–210)	180 (160–204)	11215	1514
	60–79	31 (22–38)	26 (17–35)	275 (0–1645)	942 (54–3510)	−95 (−100–88)	−93 (−98–86)	123 (101–144)	116 (94–139)	1.27 (0.89–1.74)	1.32 (0.92–1.63)	444 (382–520)	433 (363–509)	182 (138–241)	182 (133–242)	180 (161–201)	177 (158–198)	6468	2232
	80+	21 (12–30)	19 (10–28)	2057 (84–5239)	2645 (240–7342)	−93 (−97–87)	−91 (−97–85)	103 (82–128)	98 (78–124)	1.48 (1.03–1.86)	1.45 (1.09–1.94)	398 (336–478)	384 (333–459)	166 (138–219)	153 (119–202)	163 (147–178)	158 (144–175)	319	501
Women	18–39	44 (36–50)	38 (30–45)	0 (0–0)	0 (0–2)	−86 (−92–80)	−85 (−92–79)	181 (160–204)	171 (148–195)	0.24 (0.16–0.36)	0.31 (0.20–0.52)	352 (304–405)	346 (264–419)	219 (129–348)	213 (117–310)	127 (113–144)	125 (109–143)	8812	265
	40–59	34 (25–42)	28 (17–38)	0 (0–23)	12 (0–745)	−91 (−97–84)	−89 (−95–81)	155 (133–178)	144 (122–166)	0.38 (0.26–0.56)	0.48 (0.31–0.72)	346 (297–401)	349 (291–411)	246 (164–351)	234 (141–351)	130 (115–148)	132 (115–153)	14440	1324
	60–79	23 (12–32)	17 (6–27)	100 (0–1122)	757 (17–3512)	−92 (−98–86)	−91 (−97–84)	122 (103–143)	116 (95–137)	0.50 (0.35–0.71)	0.60 (0.42–0.85)	324 (276–379)	313 (262–371)	245 (172–335)	226 (152–316)	124 (110–140)	123 (108–143)	7284	2080
	80+	11 (1–20)	9 (−1–19)	1914 (127–6039)	2614 (548–6666)	−90 (−96–84)	−88 (−95–81)	99 (77–118)	93 (74–116)	0.60 (0.43–0.84)	0.62 (0.41–0.88)	294 (252–339)	271 (227–316)	205 (141–276)	193 (131–257)	116 (104–130)	116 (102–130)	534	694

Numbers are median values with interquartile ranges (IQR) in parentheses.
*Refers to chronological age of patients (not CT biological age).

Discussion

We found that a prediction model incorporating only understandable CT-based biomarkers of abdominal tissues and organs can provide a useful assessment of cardiometabolic health and estimation of longevity. This study demonstrates the value of harnessing the rich biometric tissue and organ data embedded within all body CT scans, but which typically go unused in routine practice[10,13,18]. Regardless of clinical indication, these CT scans can be opportunistically leveraged as an objective means for detecting silent or pre-symptomatic cardiometabolic conditions, including cardiovascular disease, osteoporosis, sarcopenia, diabetes, and metabolic syndrome[12–17]. When previously unsuspected, these CT findings could initiate early preventive measures. For individuals with suspected or known risk factors, the objective and visual nature of the CT biomarker display may nonetheless motivate positive action. The advent of fully automated AI-based algorithms to mimic and replace more arduous manual approaches to these CT-based measurements provides for an efficient, explainable, objective, and reproducible method that is generalizable. Since body CT scans are already performed in such high volumes in middle-aged and older adults for a wide array of reasons[19], the potential for quasi- population-based opportunistic screening already exists.

The concept of biological aging is not new, but has lately become a topic of keen public interest, as seen in the recent lay press[2–4]. Beyond just the health-conscious "worried well", there is growing recognition that many health care decisions should not be based solely on chronological age, but rather should account for the cumulative physiologic effects of lifestyle habits, genetic predisposition, and superimposed disease processes. The burgeoning interdisciplinary field of geroscience has largely focused on cellular and subcellular biomarkers, such as mitochondrial dysfunction, proteostasis, stem cell dysfunction, nutrient sensing, genomic instability, telomere dysfunction, cellular senescence, and epigenetic change[8]. These "frailomics" measures of aging will undoubtedly provide some insight, but are unlikely to fully translate to the overall state of health of tissues, organs, or most importantly, the individual patient at the organism level.

Radiologic imaging biomarkers, whether more straightforward "explainable" measures as we employ or more complex radiomics (that we avoid), have generally received little attention for their potential role in determining an effective biological age[7,9]. In fact, a recent international task force on biological aging enumerated a myriad of potential biomarkers but failed to include imaging biomarkers and radiomics[8]. However, we believe that imaging features (particularly CT-based) may better reflect the cumulative macroscopic effects of aging at the tissue and organ levels. Although numerous studies have shown a correlation between various imaging findings and patient age, comparatively few have explored the concept of biological aging[20–22]. Furthermore, we are not aware of any prior large-scale population-based studies on the order of 100,000 patients. In general, the model performed slightly better in middle-age adults compared with older adults. This may be advantageous in terms of a more opportune target age for preventive interventions.

Our findings suggest that CT-based cardiometabolic biomarkers can effectively reflect the phenotypic pathologic and senescent changes at the tissue, organ, and organism levels that result from the interaction of environmental factors on genetic predisposition. These macroscopic changes may be more relevant than (or at least complementary to) changes observed at the cellular or subcellular level. By utilizing only explainable AI algorithms, as opposed to a more "black box" radiomics methodology, we believe this transparent approach could be more readily understood and accepted by patients and adopted by healthcare providers. The explainable methodology for our CTBA model provides transparency and avoids the opaqueness of deep learning approaches. Furthermore, our feature selection process

https://doi.org/10.1038/s41467-025-56741-w

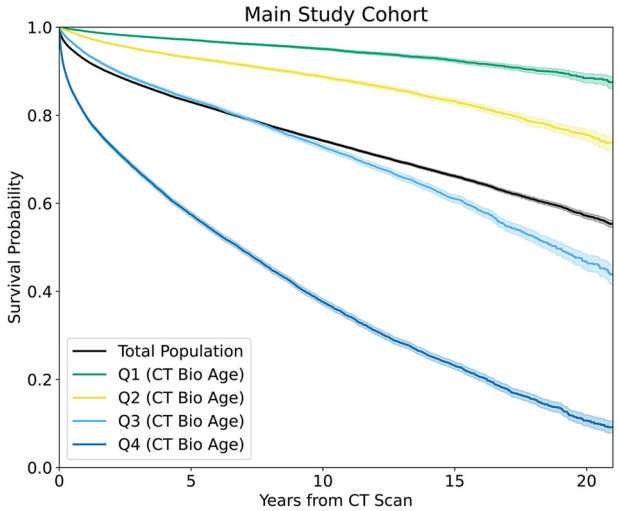

Fig. 4 | Kaplan-Meier plot for CT biological age (CTBA) model survival for the full primary study cohort ($n = 123,281$). Note the obvious separation in survival probability over time among the various CTBA risk quartiles, despite the fact that the model is blinded to demographic factors such as chronological age. Color bands reflect 95% confidence intervals.

using the IPA drop retains only biomarkers that improve predictive accuracy.

Clinical frailty assessments in current use are generally aimed more at advanced geriatric and acute care settings and tend to be somewhat onerous to execute[23]. BMI has been in use for many years as a determinant of health status but this practice is now being discouraged by the AMA and other groups. Our results reinforce the poor predictive nature of BMI. CT-based biological aging could also serve as an objective frailty assessment and could be further modified in terms of reporting for sarcopenia, myosteatosis, and fracture risk[12–17]. Our CT-based approach could also be used to augment existing clinical risk prediction models, assuming the combination provides complementary information. A number of simple online risk calculators exist, most of which are disease-specific in scope (eg, for breast or lung cancer assessment). Broader online risk calculators such as ePrognosis require manual entry of a host of demographic, clinical, and laboratory data (https://eprognosis.ucsf.edu). While these can provide for some level of risk assessment, a single CT likely provides more detailed objective insight into a patient's actual cardiometabolic status. Of course, these approaches may prove to be complementary in nature with CT-based assessment.

The fact that CT-based biomarkers of muscle density, aortic plaque burden, visceral fat, and bone mineral density contributed the most to our CT biological age model was not unexpected given their

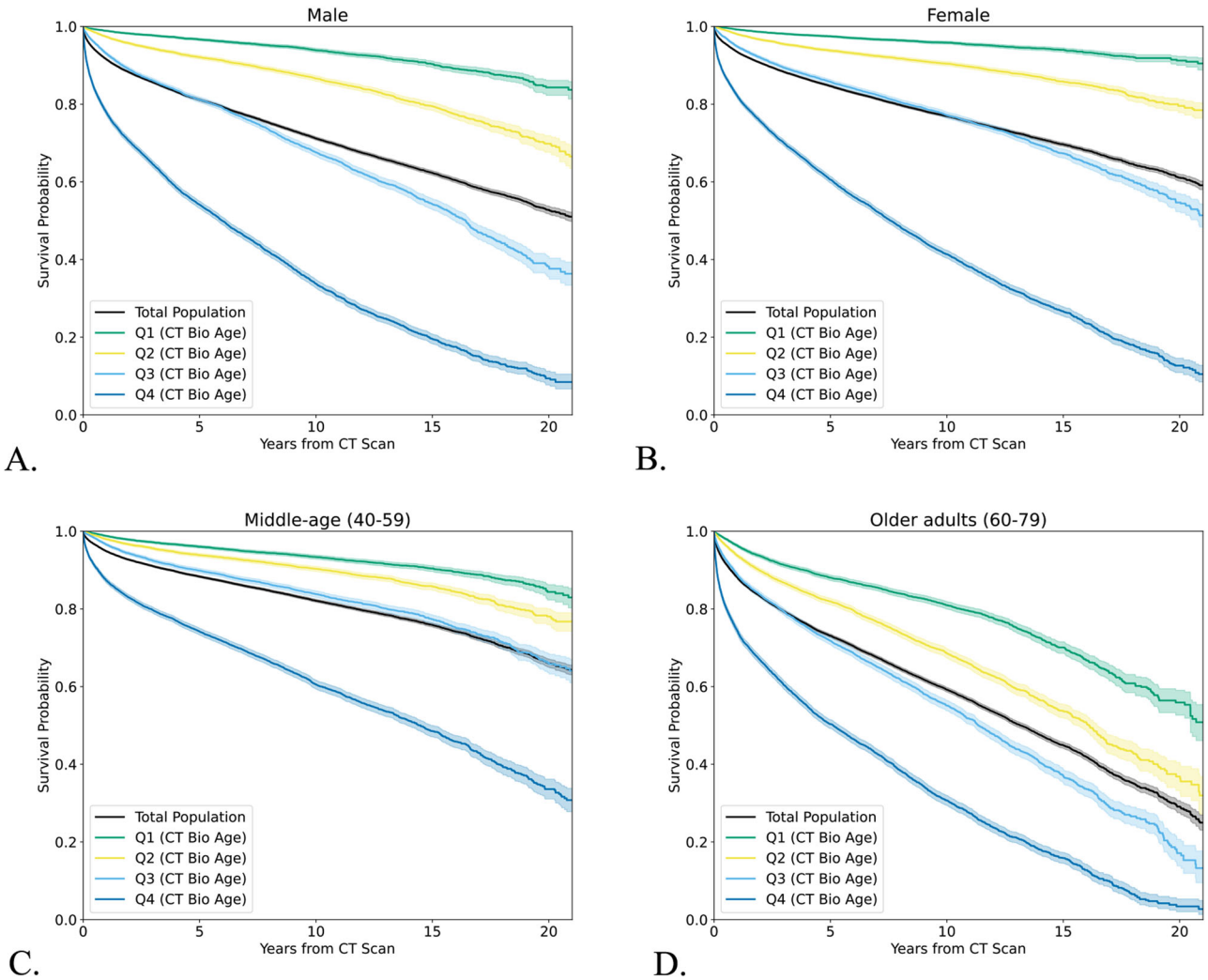

Fig. 5 | Kaplan-Meier survial plots for the patient sub-cohorts of the primary study cohort. Depicted are plots for **A** Male ($n = 64,973$), **B** Female ($n = 58,308$), **C** middle-aged (40–59 years, $n = 47,651$), and **D** older adult (60–79 years, $n = 38,973$) cohorts. Color bands reflect 95% confidence intervals.

Table 3 | Results of the CT biological age (CTBA) model

Cohort	N	5-year AUC	10-year AUC	HR*	HR**
Total Cohort	123,281	0.890 (0.884–0.896)	0.880 (0.875–0.885)	8.73 (8.14–9.36)	3.13 (3.04–3.23)
Females	58,308	0.905 (0.898–0.913)	0.889 (0.882–0.896)	8.40 (7.58–9.31)	3.08 (2.95–3.23)
Males	64,973	0.874 (0.865–0.883)	0.871 (0.863–0.878)	8.82 (8.04–9.68)	3.20 (3.07–3.33)
40–59 year-olds	47,651	0.857 (0.841–0.872)	0.842 (0.829–0.856)	7.10 (6.57–7.68)	4.33 (4.13–4.53)
60–79 year-olds	38,973	0.834 (0.824–0.844	0.816 (0.806–0.825)	5.13 (4.83–5.45)	3.26 (3.15–3.38)
Excluding Death within 2 years	111,596	0.820 (0.814–0.826)	0.838 (0.833–0.842)	17.06 (15.85–18.36)	6.09 (5.90–6.30)
Excluding Cancer within 5 years†	101,203	0.876 (0.872–0.880)	0.880 (0.877–0.884)	24.79 (22.95–26.76)	8.44 (8.18–8.71)
External Cohort	40,718	0.893 (0.867–0.918)	0.888 (0.869–0.908)	5.14 (3.98–6.63)	2.45 (2.24–2.69)

The CTBA model was constructed from CT-biomarkers only, without any input regarding chronological age, sex, or race; HRs are age- and sex-corrected for total and external validation cohorts; HRs for sex cohorts were corrected for age, whereas HRs for age cohorts were corrected for sex.
*Comparing the highest-risk CTBA quartile vs the lowest-risk quartile.
**Comparing the highest-risk CTBA quartile vs the other three quartiles.
†Cancer diagnosis within 5 years before or after CT.

Table 4 | Age-specific results of the CT biological age (CTBA) model

Cohort	N	5-year AUC	10-year AUC	HR*	HR**
40–44 year-olds	9048	0.867 (0.821–0.914)	0.832 (0.793–0.872)	6.54 (5.27–8.11)	4.41 (3.88–5.02)
45–49 year-olds	10,623	0.842 (0.807–0.878)	0.821 (0.790–0.853)	5.17 (4.40–6.07)	3.58 (3.24–3.96)
50–54 year-olds	14,257	0.845 (0.814–0.876)	0.854 (0.831–0.877)	6.62 (5.78–7.58)	4.38 (4.03–4.75)
55–59 year-olds	13,723	0.859 (0.834–0.883)	0.834 (0.812–0.855)	6.46 (5.72–7.31)	3.95 (3.66–4.26)
60–64 year-olds	12,703	0.839 (0.817–0.862)	0.826 (0.807–0.847)	3.57 (3.34–-3.83)	3.61 (3.37–3.87)
65–69 year-olds	11,226	0.847 (0.824–0.866)	0.821 (0.803–0.839)	4.62 (4.17–5.11)	3.16 (2.95–3.38)

The CTBA model was constructed from CT-biomarkers only, without any input regarding chronological age, sex, or race; HRs for these age sub-cohorts are corrected for sex.
*Comparing the highest-risk CTBA quartile vs the lowest-risk quartile.
**Comparing the highest-risk CTBA quartile vs the other three quartiles.

established relationship with cardiometabolic disease[12,13,17]. With the exception of visceral fat, these biomarkers have a well-defined relationship with age[24–26]. However, more effective biological aging likely goes beyond simple quantification of the cumulative effects of aging, but also includes inflammation and related metabolic derangements. Skeletal muscle density, which is measured at CT using attenuation values and reflects the degree of myosteatosis, was the dominant biomarker in the CTBA model, whereas muscle cross-sectional area played a very minor role. This is consistent with prior work showing that CT-based measures of muscle quality (sarcopenic myosteatosis) are significantly more predictive of survival than CT-based measures of muscle quantity (myopenia)[12]. The prognostic value of coronary calcium scoring at CT is also well established, and we have found that quantifying calcific plaque of the abdominal aorta is also a powerful biomarker for risk prediction[13,15]. Our automated aortic plaque tool also has the additional advantage that it can be applied to CT scans with IV contrast[27]. The opportunity for incidental osteoporosis screening at CT has also been recognized for over a decade[28]. However, manual case-by-case assessment in the course of routine CT interpretation has failed to move the needle like a more programmatic, automated approach would. There is evidence that the opportunistic reporting of automated quantification of atherosclerotic plaque and bone mineral density at abdominal CT would be a cost-saving measure[29]. By systematically leveraging or repurposing these incidental tissue and organ measures on CT scans, there could be substantial implications for more intelligent utilization of limited healthcare resources.

We acknowledge the limitations to our investigation. Due to the need for a large patient cohort with built-in long-term survival outcomes, this was by necessity a retrospective study. The indications for CT imaging varied widely – both a methodological strength and a weakness. However, the predictive results of the CTBA model remained robust after addressing potential issues related to imminent death, cancer diagnosis, and patient age at CT. Model robustness, however, does not imply causation. The primary patient cohort and the external validation cohort lacked substantial racial or ethnic diversity, with both comprising Midwestern U.S. populations that were approximately 90% White. We plan to address this limitation with a multicenter trial consisting of broad national and international participation. We did not consider socioeconomic factors in the demographic-based model, but we also plan to investigate this utilizing the area deprivation index (ADI), a validated measure of

https://doi.org/10.1038/s41467-025-56741-w

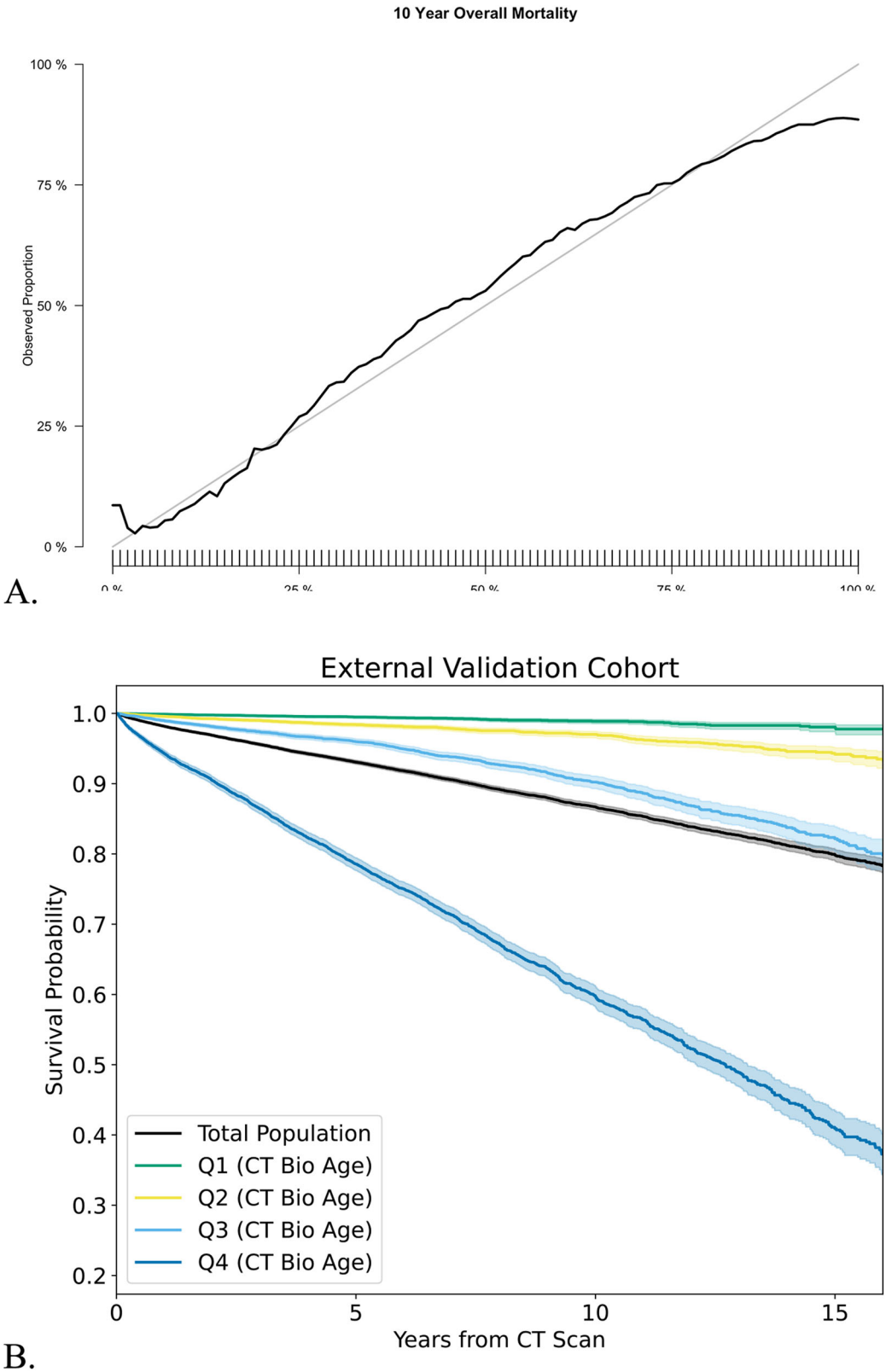

Fig. 6 | Calibration and Kaplan-Meier plots for the CTBA model applied to the external validation cohort. A The diagonal 45° line represents an ideal model in which estimates of survival are perfectly calibrated with the outcome. The black line illustrates the performance of the CTBA model, which approaches the ideal state. **B** Kaplan-Meier plot ahows clear separation among the various CTBA risk quartiles, despite the fact that demographic factors such as chronological age are not included in the model. This external cohort was composed only of outpatients and as such appeared healthier overall than the primary cohort, with improved survival despite similar mean age. Color bands reflect 95% confidence intervals.

socioeconomic disadvantage[30]. The automated AI pipeline used to obtain the CT cardiometabolic biomarkers is a research tool that is not yet commercially available. The inclusion of demographic, clinical, and laboratory measures with the CT biomarkers in a combined model would likely incrementally improve survival prediction but was beyond the scope of this work. Finally, our CT-based biological age model is based on measurable cardiometabolic and senescent factors and cannot completely account for other co-existing maladies that may impact survival, such as trauma, cancer, infection, and dementia, among others. However, when excluding patients with cancer and near-term mortality, the CT-based model proved to be even more robust.

In summary, we have shown that a CT-based biological age (CTBA) model informed only by a panel of explainable AI-derived biomarkers provides a phenotypic cardiometabolic assessment for improved and personalized prediction of remaining life expectancy over usual demographic inputs. These CT measures reflect the cumulative impact of lifestyle, genetic predisposition, and chronological aging. In addition, these objective body composition findings may reflect an early pre-symptomatic phase of disease, prior to the development of clinically recognizable findings. This valuable imaging data can be opportunistically derived from nearly any abdominal CT, whether retrospectively or prospectively and regardless of the clinical indication. Incorporating this objective biological information into the full clinical assessment might better inform downstream healthcare decisions and resource allocation.

Methods

Study design and patient cohort

This retrospective cohort study was HIPAA-compliant and approved by the IRB at UW-Madison. The need for signed informed consent was waived for this large retrospective cohort. The initial patient inclusion criteria were kept intentionally broad, consisting of any adult aged 18 years or older with an abdominal CT scan available in the PACS at the University of Wisconsin Hospital and Clinics (Madison, WI, USA) performed over a 20-year period. Patient sex was based on self-report from the electronic medical record. The patient settings for this cohort, where available, included predominately outpatients (43.6%) and the ED (41.5%), with a minority of inpatients (14.9%). To mitigate the risk of immediate mortality bias, we performed a sub-analysis after excluding all patients who died within 2 years of the CT scan. In addition, we performed an additional sub-analysis after excluding patients with a cancer diagnosis within 5 years before or after the CT scan. Further sub-analyses were also performed after restricting patient age at the time of CT to five-year windows to minimize the impact of age. We also curated an external validation cohort of outpatients from Duly Health and Care (Downers Grove, IL, USA), with CT scans also performed over a 20-year period.

For the purpose of this study, the earliest available abdominal CT scan for each patient was used, both to ensure the longest possible clinical follow-up and to minimize the impact of any subsequent treatment or interventions. Given the broad inclusion criteria, a wide variety of clinical indications for scanning at the outpatient, inpatient, and emergency department settings was observed. The specific make and model of multi-detector CT scanners are also widely varied, but these CT biomarkers algorithms have proven robust to all encountered vendors[31]. Additional CT scanning details are included in the methodology supplement. For comparison, we also recorded patient BMI closest in timing to the CT scan.

The main clinical outcome measure was patient death (all-cause mortality) or, if not deceased as of their verifiable clinical encounter, the date of last reliable contact. Acceptable encounters with medical staff included clinic visit, procedure, hospitalization, laboratory testing, and consultation. Confirmation of death for the main study cohort was periodically updated using internal and external sources, included the electronic medical record and the Social Security Death Master File.

Automated CT biomarker panel

A pipeline of mature, validated, and explainable CT-based AI algorithms automatically quantified skeletal muscle, abdominal fat, aortic calcification, bone density, liver, spleen, and kidneys, as described below and in the supplementary methods.

The panel of fully automated deep learning AI CT-based body composition algorithms used in this investigation have been integrated into a single portable Docker container at the University of Wisconsin. The individual CT body composition tools were developed, trained, and tested in separate cohorts at the NIH Clinical Center and the University of Wisconsin (see supplementary methods for details). The tools have been subsequently modified with deep-learning improvements and validated at the University of Wisconsin. Source CT data from patient scans were preprocessed and reformatted into 3 × 3-mm series, upon which the AI tools were applied to create the body composition measures.

The first step for the AI toolkit is automatic vertebral body localization using a convolutional neural network (CNN) based on the unsupervised body part regression algorithm and applied in Caffe (Fig. 1). This process is used to identify the T12 through L4 vertebral bodies levels, from which the various segmented tissue and organ composition measures (density, area, volume) are subsequently derived. For muscle measures, a U-Net model architecture was used to identify the body wall, paraspinal, and psoas musculature, including intermuscular adipose tissue. Fat and bone measures were obtained using a U-Net like architecture with VGG11 encoder to segment visceral fat, subcutaneous fat, and trabecular bone. Aortic calcification was quantified using a modified 3D U-Net architecture to determine calcified aortic plaque from the diaphragm to the aortic bifurcation. Calcification is reported as an Agatston score. Volumetric organ segmentation for the liver, spleen, and kidneys each entailed a modified 3D U-Net and CycleGAN for CNN segmentation. The specific CT body composition biomarkers included in this study are listed in Supplementary Table 1. Figure 1 depicts a schematic flowchart. In addition to the numerical output for the various CT biomarkers, QA images (Fig. 2) are derived that depicts the tissue and organ segmentation at the L1 and L3 vertebral levels, as well as a coronal maximum intensity projection (MIP) to allow for rapid visual confirmation for individual cases.

CT biological age model methodology and statistical analysis

Multivariate survival analysis was modeled using Cox proportional hazards regression. A standard demographics assessment used patient chronological age, sex, and race as the predictors, whereas the CTBA model used the CT parameters exclusively, without any demographic input. Biomarker selection for the CTBA model was performed based on the index of prediction accuracy (IPA)[32]. Individual CT biomarkers were assessed according to their "IPA drop" – the higher the drop, the more important the biomarker contribution to the CTBA model. More specifically, predictors were ranked by their smallest contribution towards the IPA and eliminated unless they contributed an IPA drop value of at least 0.1. Linearity assumptions for continuous predictors were relaxed by using restricted cubic splines with 3 knots. Predictive abilities were assessed by calculating the time-dependent areas under the receiver operating characteristic curve (AUC), as well as calibration curves[33]. These assessments of discrimination and calibration were done with use of bootstrapping (200 resamples).

Five- and 10-year AUC values were derived for the final CTBA and demographics models, as well as for BMI. Survival curves were plotted using the Kaplan-Meier estimator, splitting the CTBA model results into quartiles. Univariate and multivariate analyses of the cardiometabolic CT biomarkers were performed, with patients chronological

age, sex, and race considered as potential confounders. Age- and sex-corrected hazard ratios (HRs) with 95% CIs were computed for the CTBA model, comparing the highest-risk quartile with both the lowest-risk quartile, and with the other three quartiles. We compiled and compared summary statistics for patients who died versus survived over the course of available clinical surveillance. All analyses were performed using R version 4.3.1.

The CTBA model was not informed by demographic factors (chronological age, sex, and race), or by any acute or chronic medical conditions, such as known cardiovascular disease, diabetes, or cancer, even though this clinical information would have improved the prediction of life expectancy. Consequently, this model was based solely on the CT biomarkers. A nomogram for this standalone model of individual CT biomarkers contributing to the CTBA model was generated. A calibration plot was constructed to compare the CTBA model survival estimates for the external validation cohort against the ideal state.

Reporting summary

Further information on research design is available in the Nature Portfolio Reporting Summary linked to this article.

Data availability

The study protocol and data will be readily shared upon request for reproducibility purposes. Responses will be made within one month of receipt. Access to the data used for this study will be made available, subject to an internal review by the authors' institution to ensure that participant privacy is protected, and subject to completion of a data sharing agreement, approval from the institutional review board of UW-Madison, and in accordance with the current data sharing guidelines of UW-Madison and The University of Wisconsin School of Medicine & Public Health. Please submit such requests to J. W. G. (JGarrett@uwhealth.org). Source data are provided with this paper.

Code availability

The statistical code will be readily shared upon request for reproducibility purposes, following review by the authors and approval by the information security office at the University of Wisconsin School of Medicine & Public Health. Responses will be made within one month of receipt. Please submit such requests to J.W. (JGarrett@uwhealth.org).

References

1. Levine, M. E. Modeling the rate of senescence: can estimated biological age predict mortality more accurately than chronological age? *J. Gerontol. Ser. A, Biol. Sci. Med. Sci.* **68**, 667–674 (2013).
2. Attia, P., Gifford B. *Outlive: the Science & Art of Longevity.*, (Harmony Books, 2023).
3. Smith, D. G. What's Your 'Biological Age'? New tests promise to tell you if you have the cells of a 30-year-old or a 60-year-old. in *The New York Times* (The New York Times, https://www.nytimes.com/2023/12/19/well/live/biological-age-testing).
4. Janin, A. To Get Ahead of Diseases, It May Help to Find Your Organ Age. in *The Wall Street Journal* (The Wall Street Journal, https://www.wsj.com/health/wellness/aging-biological-age-organs-health).
5. Comfort, A. Test-battery to measure ageing-rate in man. *Lancet* **2**, 1411–1414 (1969).
6. Oh, H. S. et al. Organ aging signatures in the plasma proteome track health and disease. *Nature* **624**, 164–172 (2023).
7. Li, Z. et al. Progress in biological age research. *Front Public Health* **11**, 1074274 (2023).
8. LeBrasseur, N. K. et al. Identifying Biomarkers for Biological Age: Geroscience and the ICFSR Task Force. *J. Frailty aging* **10**, 196–201 (2021).
9. Bafei, S. E. C. & Shen, C. Biomarkers selection and mathematical modeling in biological age estimation. *NPJ Aging* **9**, 13 (2023).
10. Pickhardt, P. J. Value-added opportunistic CT screening: state of the art. *Radiology* **303**, 241–254 (2022).
11. Pickhardt, P. J. et al. Opportunistic screening at abdominal CT: Use of automated body composition biomarkers for added cardiometabolic value. *Radiographics* **41**, 524–542 (2021).
12. Nachit, M., Horsmans, Y., Summers, R. M., Leclercq, I. A. & Pickhardt, P. J. AI-based CT body composition identifies myosteatosis as key mortality predictor in asymptomatic adults. *Radiology* **307**, e222008 (2023).
13. Pickhardt, P. J. et al. Automated CT biomarkers for opportunistic prediction of future cardiovascular events and mortality in an asymptomatic screening population: a retrospective cohort study. *Lancet Digit. Health* **2**, E192–E200 (2020).
14. Pickhardt, P. J. et al. Utilizing fully automated abdominal CT-based biomarkers for opportunistic screening for metabolic syndrome in adults without symptoms. *Am. J. Roentgenol.* **216**, 85–92 (2021).
15. O'Connor, S. D., Graffy, P. M., Zea, R. & Pickhardt, P. J. Does nonenhanced CT-based quantification of abdominal aortic calcification outperform the framingham risk score in predicting cardiovascular events in asymptomatic adults? *Radiology* **290**, 108–115 (2019).
16. Liu, D. et al. Fully automated CT imaging biomarkers for opportunistic prediction of future hip fractures. *Br. J. Radiol.* (2024).
17. Pickhardt, P. J. et al. Automated abdominal CT imaging biomarkers for opportunistic prediction of future major osteoporotic fractures in asymptomatic adults. *Radiology* **297**, 64–72 (2020).
18. Pickhardt, P. J. et al. Opportunistic screening: radiology scientific expert panel. *Radiology* **307**, e222044 (2023).
19. Moreno, C. C. et al. Changing abdominal imaging utilization patterns: perspectives from medicare beneficiaries over two decades. *J. Am. Coll. Radio.* **13**, 894–903 (2016).
20. Jonsson, B. A. et al. Brain age prediction using deep learning uncovers associated sequence variants. *Nat. Commun.* **10**, 5409 (2019).
21. Rule, A. D. et al. Older tissue age derived from abdominal computed tomography biomarkers of muscle, fat, and bone is associated with chronic conditions and higher mortality. *Mayo Clin Proc* (2024).
22. Raghu, V. K., Weiss, J., Hoffmann, U., Aerts, H. & Lu, M. T. Deep learning to estimate biological age from chest radiographs. *JACC. Cardiovasc. Imaging* **14**, 2226–2236 (2021).
23. Church, S., Rogers, E., Rockwood, K. & Theou, O. A scoping review of the Clinical Frailty Scale. *BMC Geriatr.* **20**, 393 (2020).
24. Jang, S. et al. Opportunistic osteoporosis screening at routine abdominal and thoracic CT: Normative L1 trabecular attenuation values in more than 20,000 adults. *Radiology* **291**, 360–367 (2019).
25. Graffy, P. M. et al. Deep learning-based muscle segmentation and quantification at abdominal CT: application to a longitudinal adult screening cohort for sarcopenia assessment. *Bri. J. Radiol.*, 20190327 (2019).
26. Graffy, P. M., Liu, J., O'Connor, S., Summers, R. M. & Pickhardt, P. J. Automated segmentation and quantification of aortic calcification at abdominal CT: application of a deep learning-based algorithm to a longitudinal screening cohort. *Abdom. Radio.* **44**, 2921–2929 (2019).
27. Summers, R. M. et al. Atherosclerotic Plaque burden on abdominal CT: Automated assessment with deep learning on noncontrast and contrast-enhanced scans. *Acad. Radio.* **28**, 1491–1499 (2021).
28. Pickhardt, P. J. et al. Opportunistic screening for osteoporosis using abdominal computed tomography scans obtained for other indications. *Ann. Intern. Med.* **158**, 588–595 (2013).
29. Pickhardt, P. J., Correale, L. & Hassan, C. AI-based opportunistic CT screening of incidental cardiovascular disease, osteoporosis, and sarcopenia: cost-effectiveness analysis. *Abdom. Radiol.* **48**, 1181–1198 (2023).

30. Lee, M. H., Zea, R., Garrett, J. W., Summers, R. M. & Pickhardt, P. J. AI-generated CT body composition biomarkers associated with increased mortality risk in socioeconomically disadvantaged individuals. *Abdom. Radiol.* (2024).
31. Pooler, B. D., Garrett, J. W., Southard, A. M., Summers, R. M. & Pickhardt, P. J. Technical adequacy of fully automated artificial intelligence body composition tools: assessment in a heterogeneous sample of external CT examinations. *Ajr. Am. J. Roentgenol.* **221**, 124–134 (2023).
32. Kattan, M. W. & Gerds, T. A. The index of prediction accuracy: an intuitive measure useful for evaluating risk prediction models. *Diagn. Progn. Res.* **2**, 7 (2018).
33. Harrell, F. E., Jr., Lee, K. L. & Mark, D. B. Multivariable prognostic models: issues in developing models, evaluating assumptions and adequacy, and measuring and reducing errors. *Stat. Med.* **15**, 361–387 (1996).

Acknowledgements

Supported in part by the Intramural Research Program of the National Institutes of Health Clinical Center.

Author contributions

P.J.P. conceived the study and prepared the manuscript, J.W.G. and R.M.S. created and implemented the AI tools, M.W.K. created the CT biological age model and performed statistical analyses with R.Z., M.H.L., B.D.P., and D.L. supported data organization and analysis, A.P. organized the external cohort, and all authors edited the manuscript.

Competing interests

P.J.P.: advisor to Bracco Diagnostics, GE HealthCare, Nanox-AI, and ColoWatch; stock options, ColoWatch; J.W.G.: Advisor to RadUnity, Shareholder in NVIDIA; R.M.S.: Royalties from iCAD, ScanMed, Philips, Translation Holdings, PingAn, MGB; research support through a CRADA with PingAn. The remaining authors declare no competing interests.

Additional information

Supplementary information The online version contains supplementary material available at https://doi.org/10.1038/s41467-025-56741-w.

Correspondence and requests for materials should be addressed to Perry J. Pickhardt.

Peer review information *Nature Communications* thanks Samaneh Farsijani, David Furman and Shayan Mostafaei for their contribution to the peer review of this work. A peer review file is available.